

2

Non-oxide (Silicon Carbide) Fibers

James A. DiCarlo and Hee-Mann Yun

NASA Glenn Research Center

21000 Brookpark Road

Cleveland, Ohio 44135

Phone 216-433-5514

James.A.DiCarlo@NASA.gov

ABSTRACT

Non-oxide ceramic fibers are being considered for many applications, but are currently being developed and produced primarily as continuous-length structural reinforcement for ceramic matrix composites (CMC). Since only those fiber types with compositions based on silicon carbide (SiC) have demonstrated their general applicability for this application, this chapter focuses on commercially available SiC-based ceramic fiber types of current interest for CMC and on our current state of experimental and mechanistic knowledge concerning their production methods, microstructures, physical properties, and mechanical properties at room and high temperatures. Particular emphasis is placed on those properties required for successful implementation of the SiC fibers in high-temperature CMC components. It is shown that significant advances have been made in recent years concerning SiC fiber production methods, thereby resulting in pure near-stoichiometric small-diameter fibers that provide most of the CMC fiber property requirements, except for low cost.

1. INTRODUCTION

Continuous-length polycrystalline ceramic fibers with non-oxide compositions are currently being developed and used for a variety of low and high-temperature structural applications. Recent literature reviews detail the process methods, properties, and applications for the many non-oxide fiber types that have been developed over the last 30 years [1–5].

In practically all cases, the non-oxide fiber types have compositions based on silicon compounds such as silicon carbide (SiC) and silicon nitride (Si_3N_4). The application currently envisioned as the most important for these fiber types is that of structural reinforcement of ceramic matrix composites (CMC) with upper use temperatures well above the current capability of structural metallic alloys ($> 1100^\circ\text{C}$). However, only the SiC-based types have reached the stage in which they have been used to reinforce different high-temperature CMC systems, and as such have composite property databases available in the open literature in order to verify their reinforcement capabilities. Thus the focus of this chapter is to present key performance-related properties of these commercial SiC-based fiber types since they have demonstrated their general applicability as CMC reinforcement. To this end, the first section presents information on the key production details and as-produced properties of the SiC types as individual fibers and on our current understanding concerning the underlying process-microstructure-property relationships. The second section presents available data concerning how the deformation and fracture properties of the individual fibers are affected by temperature, time, stress, and oxidizing environments, again with a discussion of underlying mechanisms. Finally, the last section discusses how these and other SiC fiber properties are affecting the technical implementation of advanced high-temperature ceramic matrix composites.

2. APPLICATIONS

Research and development efforts over recent years have focused on achieving SiC-based ceramic fibers with the optimum intrinsic and extrinsic thermostructural properties required as reinforcement of high-temperature CMC components, such as those used in the hot-sections of engines for power and propulsion. As such, general first-level fiber property requirements are the ability to display high tensile strength in its as-produced condition, and the ability to retain as much of this strength as possible at high temperatures for long times under high stresses and oxidizing environmental conditions. For strength retention, key goals are achieving thermally stable microstructures that display high creep resistance and high oxidation resistance. However, there are also a variety of second-level fiber property requirements that are related to CMC fabrication and service. These include the need for small diameter, carbon-free surfaces, low roughness surfaces, high intrinsic thermal conductivity, and low acquisition cost.

3. PROCESSING

Today the most common approach for producing polycrystalline ceramic fibers is by spinning and heat treating chemically derived precursors. In the case of SiC-based fibers, “green” fibers are spun from organo-metallic “preceramic” polymer precursors, such as polycarbosilane, followed by cross-linking (curing) and heat treatment steps, such as pyrolysis and sintering, to convert the fibers to ceramic materials typically based on β -phase SiC [4]. Particular process and compositional details for a variety of SiC fiber types are discussed in the next section.

A key characteristic of the polymer-derived SiC fibers is their ultra-fine microstructure with grain sizes in the nanometer range. Fine grains are typically required for good

tensile strength, but can be detrimental to creep resistance [6]. The use of polymer technology also allows the commercial preparation of SiC fibers with small diameters ($<15\text{ }\mu\text{m}$) and in the form of continuous-length multi-fiber tows, which are then typically coated with thin polymer-based sizings before being supplied to customers on ~ 100 gram spools. The sized tows with the small diameter fibers are flexible and generally easy to handle so that they can be textile-formed into fabrics, tapes, braids, and other complex shapes. Many small-diameter SiC fiber manufacturers also supply fibers in fabric form since most composite fabrication processes used today generally require an initial step of fabric stacking or lay-up into a near net-shaped architectural preform of the final CMC product. Although there are no current methods for fabricating continuous-length single-crystal SiC fibers, it is expected that the small-diameter polycrystalline SiC fibers will always display better handle-ability and significantly lower production costs, but reduced creep resistance and temperature capability. Thermostructural capability and thermal conductivity may also be degraded in the polycrystalline SiC fibers by the presence of second phases in the fiber grain boundaries.

Polycrystalline SiC fibers in the form of continuous-length monofilaments are also being produced by the chemical vapor deposition (CVD) route, which typically uses methyl-trichlorosilane to vapor deposit fine columnar-grained ($\sim 100\text{ nm}$ long) SiC onto a resistively-heated small-diameter ($\sim 30\text{ }\mu\text{m}$) carbon monofilament that continuously passes through a long glass reactor [1]. CVD SiC fibers on small-diameter ($\sim 13\text{ }\mu\text{m}$) tungsten monofilaments are also commercially available, but due to high-temperature reactions between the SiC and tungsten, these fibers are more suitable as reinforcement of low and intermediate temperature composite systems. Although the CVD SiC fibers have displayed very high strengths ($\sim 6\text{ GPa}$ for the Ultra SCS fiber), the final fibers currently display diameters greater than $50\text{ }\mu\text{m}$, which are not conducive to fiber shaping into complex architectural preforms. Laboratory attempts have been made to reduce their diameters and to produce multi-fiber tows, but issues still exist concerning finding substrate filaments with the proper composition and diameter, methods for spreading these filaments during deposition to avoid fiber-to-fiber welding, and low-cost gas precursors for the CVD SiC.

4. PROPERTIES

4.1. As-Produced Physical and Mechanical Properties

Table 1 lists some key production and compositional details for a variety of SiC-based fiber types of current interest and availability as CMC reinforcement. The polymer-derived types range from first-generation fibers with very high percentages of oxygen and excess carbon, such as Nicalon and Tyranno Lox M, to the more recent near-stoichiometric (atomic C/Si ≈ 1) fibers, such as Tyranno SA and Sylramic. For the CVD-derived types, such as the SCS family with carbon cores, the only compositional variables in the SiC sheaths are slight excesses of free silicon or free carbon. Table 2 lists some of the key physical and mechanical properties of the SiC fiber types in their as-produced condition, as well as estimated commercial cost per kilogram, all properties important to fiber application as CMC reinforcement. These SiC fiber properties in Tables 1 and 2 are in most part those published by the indicated commercial vendors. It should be noted that the Sylramic fiber

TABLE 1. Production and Compositional Details for SiC-Based Fiber Types

Trade-Name	Manufacturer	Production Method	Elemental Composition, weight %	Approx. Maximum Production Temp.	~Grain Size, nm (~surface roughness)	Surface composition	Avg. Diam. μm	Fibers Per Tow
Nicalon, NL200	Nippon Carbon	Polymer	56 Si + 32 C + 12 O	1200°C	2	Thin carbon	14	500
Hi-Nicalon	Nippon Carbon	Polymer + Electron irr.	62 Si + 37 C + 0.5 O	1300°C	5	Thin carbon	14	500
Hi-Nicalon Type S	Nippon Carbon	Polymer + Electron irr.	69 Si + 31 C + 0.2 O	1600°C	100	Thin carbon	12	500
Tyranno Lox M	Ube Industries	Polymer	55 Si + 32 C + 10 O + 2.0 Ti	1200°C	1	Thin carbon	11	400/800
Tyranno ZMI	Ube Industries	Polymer	57 Si + 35 C + 7.6 O + 1.0 Zr	1300°C	2	Thin carbon	11	400/800
Tyranno SA 1-3	Ube Industries	Polymer + Sintering	68 Si + 32 C + 0.6 Al	>1700°C	200	Thin carbon	10 – 7.5	800/1600
Sylramic	(Dow Corning) COI Ceramics	Polymer + Sintering	67 Si + 29 C + 0.8 O + 2.3 B + 0.4 N + 2.1 Ti	>1700°C	100	Thin carbon + B + Ti	10	800
Sylramic-iBN	COI Ceramics + NASA	Polymer + Sintering + Treatment	Sylramic	>1700°C	>100	Thin in-situ BN (~100 nm)	10	800
SCS-6-9/Ultra SCS	Specialty Materials	CVD on ~30 μm C core	70 Si + 30 C + trace Si + C	1300°C	~100 by ~10	SiC/Thin carbon	140 – 70/140	mono-filament

TABLE 2. Property and Cost Details for SiC-Based Fiber Types

Trade-Name	Manufacturer	Density, g/cm ³	Avg. R.T. Tensile Strength GPa	R.T. Tensile Modulus GPa	R.T. Axial Thermal Conduct. W/m K	Thermal Expansion, ppm/°C (to 1000°C)	Current Cost, (<5Kg), \$/Kg
Nicalon, NL200	Nippon Carbon	2.55	3.0	220	3	3.2	~2000
Hi-Nicalon	Nippon Carbon	2.74	2.8	270	8	3.5	8000
Hi-Nicalon Type S	Nippon Carbon	3.05	~2.5	400-420	18		13000
Tyranno Lox M	Ube Industries	2.48	3.3	187	1.5	3.1	1500/1000
Tyranno ZMI	Ube Industries	2.48	3.3	200	2.5		1600/1000
Tyranno SA 1-3	Ube Industries	3.02	2.8	375	65		~5000
Sylramic	(Dow Corning) COI Ceramics	3.05	3.2	~400	46	5.4	10000
Sylramic-iBN	COI Ceramics + NASA	3.05	3.2	~400	>46	5.4	>10000
SCS-6-9/Ultra SCS	Specialty Materials	~3	~3.5 /~6	390-350/390	~70	4.6	~9000

type is no longer being produced by Dow Corning, but by ATK COI Ceramics, who is also producing its derivative, the Sylramic-iBN fiber.

Examining the SiC fiber properties in more detail, it can be seen that there exists a strong correlation for each fiber type between its production conditions, its final as-produced microstructure, and its as-produced physical and mechanical properties. For example, the approximate maximum production temperature of 1200°C for the first generation polymer-derived Nicalon and Tyranno Lox M fibers is typically dictated by the fact that during the green fiber curing stage, a significant amount of oxygen is introduced into the fibers. This gives rise to oxy-carbide impurity phases in the fiber microstructures, which tend to decompose into gases that volatilize from the fiber near 1200°C, thereby creating porosity and less than optimum fiber tensile strength [4]. Thus for the first generation fiber types, the high oxygen content of ~10 weight % tends to limit fiber thermal capability for strength retention and for CMC fabrication to temperatures less than 1300°C, and for CMC long-term service to temperatures less than 1200°C. The low production temperature also results in very fine grains (<5 nm), thereby contributing to high creep rates for these fiber types, which are even further enhanced by the oxygen content in the grain boundaries. In addition, in comparison to the purer near-stoichiometric SiC fibers, the oxygen and carbon content of these first generation fibers contribute to lower fiber density, elastic modulus, thermal expansion, and thermal conductivity, which is further degraded by the small grain size. On the positive side, the simplicity of the production methods for these fiber types in combination with their low production temperatures, allow these fibers to be available at the lowest cost in comparison to the other higher performing SiC fiber types.

Since it is often desirable to fabricate and to achieve long-term use of CMC above 1200°C, advanced production methods that limit the oxide phases in polymer-derived SiC fibers have recently been developed. In one method, oxygen pickup in the microstructure is reduced significantly by green fiber curing under electron irradiation. The Hi-Nicalon and Hi-Nicalon Type S fiber types from Nippon Carbon are produced by this method, and thus show much reduced oxygen content in comparison to the original Nicalon fiber [4]. The lower oxygen content allows the Hi-Nicalon Type S fiber to be produced near 1600°C, but the Hi-Nicalon fiber production temperature is limited to ~1300°C because of higher oxygen content and significant carbon content. Reducing oxygen increases fiber density, modulus, expansion, and conductivity over the original Nicalon fiber, but the high carbon content of the Hi-Nicalon fiber limits these increases. Also the higher production temperatures for both fiber types are revealed in larger grain sizes, which also impacts fiber thermal conductivity. Finally, removal of oxygen by electron irradiation appears to introduce added production costs since the Hi-Nicalon types are 4 to 6 times more expensive than the Nicalon fiber.

In another low-oxygen method, residual oxide-based impurities in the green fibers are allowed to decompose during subsequent fiber heat-treatment above 1200°C. But by introducing boron or aluminum sintering aids into the low-strength fiber microstructure and heating to temperatures above 1600°C, the remaining small SiC grains are allowed to sinter and grow, forming a fairly dense fiber with reasonable tensile strength [4]. The resulting fibers such as the Tyranno SA fiber (aluminum aids) and the Sylramic fiber (boron aids) are nearly oxygen-free and stoichiometric, with the latter type displaying the higher as-produced tensile strength. In comparison to the other fiber types with lower production temperatures, the final sintered fibers contain larger grains that are beneficial for improved fiber creep resistance and thermal conductivity, but can cause fiber strength to degrade below 3 GPa

if allowed to grow beyond ~ 200 nm in size. Also, the larger grain sizes typically result in rougher fiber surfaces, which can cause fiber-fiber abrasion in multi-fiber tows. In addition, the sintering aids can be somewhat detrimental to fiber creep and oxidation resistance. Nevertheless, the sintering approach has the major advantage of producing strong fibers at very high production temperatures, which can significantly open the temperature window for CMC fabrication and service without experiencing microstructural instabilities in the fiber reinforcement. In addition, for the Sylramic fiber type, the boron sintering aids can be removed from the fiber surface and bulk by a post-process thermal treatment in nitrogen-containing gas, giving rise to the “Sylramic-iBN” fiber that is not only creep and oxidation resistant, but contains a thin protective in-situ grown BN coating on the fiber surface [7]. But for all the sintered fiber types, fiber density and modulus are near the maximum values for SiC, which can have a negative effect, respectively, on CMC weight and on the formability of CMC fiber architectures. In addition, there is the general increase in cost for the sintered fibers that typically accompanies their higher production temperatures.

In contrast to the polymer-derived SiC fibers, the CVD SiC monofilament fibers have the production advantage of rapid high-temperature layer-by-layer formation of the SiC microstructure without the introduction of deleterious oxide phases. However, the mechanisms for SiC formation from silicon and carbon-containing chemical precursors are very complicated and quite sensitive to a number of parameters including reactant gas species, carrier and/or reducing gases, deposition pressure, temperature, gas phase concentrations, flow rate, etc.. A stoichiometric SiC microstructure may be produced locally, but is difficult to achieve throughout the entire fiber. For example, current-production CVD SiC monofilament fibers on carbon generally experience process temperatures that decrease from ~ 1500 to $\sim 1200^\circ\text{C}$ as they pass through the reactor. These conditions result in a slightly silicon-rich microstructure in the outer layers of the SiC sheath of the SCS-6 fiber, which in turn leads to fiber creep and strength instabilities at temperatures above 800°C [1]. Recently, the newer Ultra SCS fiber was developed at Specialty Materials, which displays slightly carbon-rich sheath compositions, leading to improved as-produced strength, creep resistance, and strength retention at high temperatures. Despite these small variations in stoichiometry, the SiC sheaths of the CVD fibers display physical and mechanical properties that are closest to those expected from pure β -SiC for any of the SiC fiber types. However, due to the carbon monofilament substrate, the CVD SiC fibers are ceramic composites in themselves; so that some of the fiber properties, such as density and axial modulus, are dependent on substrate size and composition. In addition, costs for current-production CVD SiC monofilaments are quite high at about \$10,000 per kilogram.

Finally, it is interesting to note in Tables 1 and 2 that, whereas fiber physical and deformation properties can be correlated with as-produced fiber composition and grain size, there is much less correlation between fiber microstructural conditions and fiber tensile strength, which is typically measured at a gauge length of 25 mm.. This non-correlation is generally to be expected since the as-produced strengths of ceramic materials are controlled by any pores or other flaws introduced into the ceramic bulk or surface during consolidation. However, in many cases for large-grained ceramics, these flaws relate in a crude manner with the inverse square root of the grain size (Griffith's law), so that ceramic strength should increase with smaller grain size. For the SiC fibers, this relationship appears to hold for average grain sizes above ~ 100 nm, based on the limited grain size variation between the Tyranno SA fibers at ~ 200 nm and the Sylramic and SCS fibers at ~ 100 nm. However,

below 100 nm, all polymer-derived fibers, despite nanometer grain sizes, show a wide variation in strength with none ever exceeding ~ 3 GPa. This observation has generally been explained by the fact that inherent in the polymer preparation and filtering processes, potential flaw-related particles with sizes of the order of ~ 100 nm are allowed to pass into the green fibers, so that these particles rather than the fiber grains are strength limiting. Another related point is that these fiber types typically have carbon-rich surface layers (see Table 1) that are capable of blunting strength-controlling fiber surface flaws; so that if the carbon is removed during CMC fabrication or service, fiber strength losses up to 20% have been observed. Thus although it would be highly desirable to develop stronger small-diameter SiC fibers, upper limit strengths of ~ 3 GPa may be all that can be currently achieved by current polymer-derived fiber production methods.

4.2. Temperature-Dependent Mechanical Properties

With increasing temperature, SiC fiber bulk properties such as elastic modulus and thermal conductivity decrease slowly in a relative manner closely equivalent to the same properties of bulk monolithic SiC. Thus it can be assumed that fiber elastic modulus E should decrease with temperature T (Celsius) by the following relationship for monolithic SiC:

$$E(T) = E_0 - [A \cdot T] \quad A = 0.020 \text{ GPa}/^\circ\text{C} \quad (1)$$

where E_0 is the fiber modulus at 0°C . This modulus behavior should extend to high temperatures, but perceived deviations could begin as low as 800°C where fiber creep strain begins to appear and to add to the fiber elastic strain. The tensile strength of SiC fibers also shows a slow monotonic decrease with temperature up to the beginning of the creep regime. However, within this regime, factors such as grain size, impurity content, and prior thermostructural history have a significant impact on the rate of fiber strength degradation with time and temperature. Thus, to better understand SiC fiber capability as structural reinforcement of high-temperature CMC, one needs to examine available data concerning the effects of temperature, time, stress, and environment on the creep and rupture behavior of the various SiC fiber types.

A convenient approach for evaluating both fiber creep behavior and rupture behavior is by the stress rupture test in which individual small-diameter fibers are dead-weight loaded under constant stress, temperature, environment, and gauge-length test conditions, and fiber creep strain is measured versus time until rupture occurs [8]. Under these conditions at high temperatures, most SiC fibers in their as-produced condition display a large transient creep stage. This can be seen in Fig. 1 for high-temperature SiC fiber types under an applied stress of 275 MPa at 1400°C in air [7]. These curves show that the creep rates for many of the fibers continuously decrease with time until rupture (letter F), giving the appearance of only primary stage creep. Although detailed mechanistic studies still need to be performed, it would appear that the transient behavior is caused by a variety of process-related factors. For example, due to production temperatures that do not exceed $\sim 1300^\circ\text{C}$, the Hi-Nicalon fibers contain very fine grains and thermally unstable oxy-carbide second phases. During long-term creep testing at 1200°C and above, it is likely that the grains grow and the creep-prone oxy-carbide phases decompose, resulting in a concurrent reduction in creep rate. These mechanisms are supported by studies in which a reduced transient stage and overall

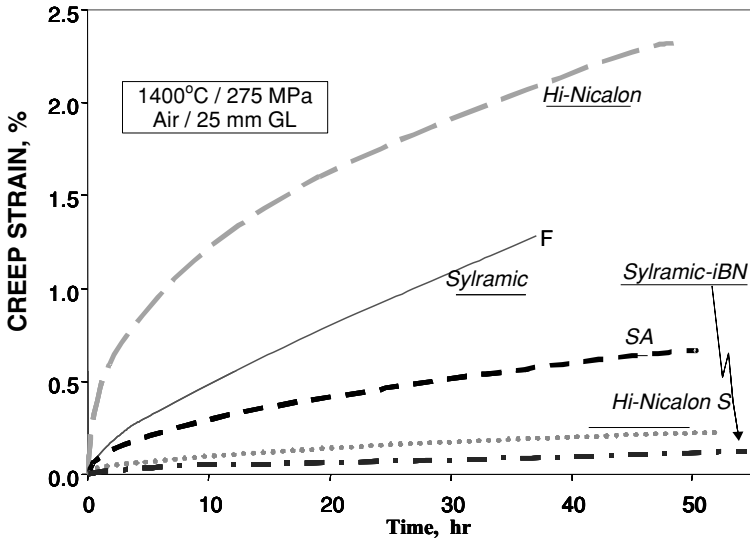


FIGURE 1. Typical creep strain versus time curves for high-temperature SiC fibers tested in air under stress-rupture conditions (F = rupture).

improvement in creep resistance were observed after thermal treatment of the Hi-Nicalon fiber type at its production temperature and above [9, 10].

For the SiC fibers with the largest grains (~ 100 to 200 nm), a variety of creep recovery and annealing studies have been performed to better understand their transient behavior. For example, recovery tests on the SCS-6 fiber show that the total creep strain typically consists of an anelastic or recoverable component plus a viscous or non-recoverable component [11]. Generally the viscous component continues to increase with time, while the anelastic component saturates with time to a value no greater than ~ 2 times the initial elastic component [12]. Based on this behavior, the anelastic component can be attributed to Zener grain-boundary sliding [13]. Thus at least a part of the transient behavior observed in Fig. 1 is due to a recoverable creep component. When the large-grained SCS-6 and Sylramic fibers were annealed for extended times near their production temperatures, grain size did not change. However, total creep strain decreased for the same test conditions, with the primary stage diminishing more rapidly than the secondary stage. Since these fiber types contain creep-prone phases, such as free silicon and boron, respectively (see Table 1), the improved creep resistance can be attributed to the elimination or minimization of these second phases from grain boundaries. Indeed, the improved creep behavior of the Ultra SCS fiber relative to the first-generation SCS-6 fiber [6] can be explained by elimination of free silicon. Likewise, the improved creep resistance of the Sylramic-iBN fiber can be attributed to boron removal from the Sylramic fiber [7]. Thus for the Fig. 1 test conditions, the transient creep behavior of as-produced SiC-based fibers can in part be explained by anelastic grain-boundary sliding and in part by unstable grain sizes and mobile second phases.

To gain a mechanistic understanding of SiC fiber creep, it is of interest to examine the property of fiber creep strength. This property is defined as the applied stress required to

allow a certain creep strain limit to be reached in a given time or service life at a given service temperature. *Thus the higher the fiber creep strength, the greater the fiber's creep resistance and ability to retain dimensional stability for a particular service application.* Under conditions where only one grain-boundary diffusion mechanism dominates, fiber creep strength σ_c can generally be described by the following relationship [14]:

$$\sigma_c^n = A_0^{-1} d^m \dot{\epsilon}_c \exp[Q_c/RT]. \quad (2)$$

Here A_0 is a composition-dependent diffusion constant; n is the creep stress exponent, d is average grain size, m is the grain size exponent, Q_c is the controlling creep activation energy, R is the universal gas constant (8.314 J/mol-K), and T is absolute temperature. If the concentration of vacancies supporting grain-boundary diffusion is not limited, creep occurs by Coble creep in which $n = 1$ and $m = 3$. However, if the concentration of vacancies is limited in the grain boundaries, for example, by the presence of second phases, interface-controlled diffusional (ICD) creep would occur with n values ranging from 2 to as high as 3. Also ICD is characterized by a much smaller dependence on grain size with $m \approx 1$ and energy Q_c greater than that for Coble creep.

Notwithstanding the existence of transient behavior for the as-produced SiC-based fibers, Fig. 2 can be constructed to examine the creep strength versus grain size dependence of these fibers both in their as-produced condition (open points) and after creep strength improvement by second phase removal (closed points) [6]. Here the selected conditions are 0.4 % total creep strain in 10 hours at 1400°C in air. In the previous discussion, it was seen that n values greater than unity are an indication of ICD creep, which in turn implies $m = 1$. Assuming this to be the case for the SiC-based fibers, one can draw the solid line in Fig. 2 near the points of the most creep-resistant fibers to suggest that ICD behavior exists in these fibers with $m/n = 1/2$, so that $n = 2$, a stress exponent typically observed for creep of polymer-derived SiC fibers [6]. Thus at the present time, the solid line in Fig. 2 represents the best creep strength behavior to be expected for SiC-based fiber types under the selected test conditions. This line shows that the annealed Sylramic fiber at ~ 100 nm grain size (i.e., the Sylramic-iBN fiber), probably represents the best SiC fiber type in terms of displaying the highest values for both creep strength and as-produced tensile strength.

For some applications, large fiber creep strains may be tolerable so that the prime concern is to assure that the fiber does not fracture or rupture during service. Typically during stress-rupture testing, the rupture time results show considerable scatter [15], so that data trends become difficult to analyze mechanistically. Nevertheless, it is possible to average the applied stresses that cause a given fiber type to rupture at a given time to develop best fit curves of applied stress or rupture strength versus time at a given temperature. For example Fig. 3 presents such stress-rupture curves for many of the same fiber types in Fig. 1 [7]. Here the test conditions are again 1400°C, air environment, and single fiber gauge lengths of ~ 25 mm. Comparing Figs. 1 and 3, one can see a general correlation between good creep-resistance and high rupture strength or long rupture time. But as explained below, this correlation may not always exist.

To simplify SiC fiber rupture behavior for technical application and mechanistic understanding, two simple empirical approaches often used for metals and ceramics have been successfully developed. One approach is by use of Larson-Miller (LM) master curves or, equivalently, thermal-activation q -maps [16]. For this approach, measurements have been made on single fibers across a time range from ~ 0.01 to over 100 hours using three types

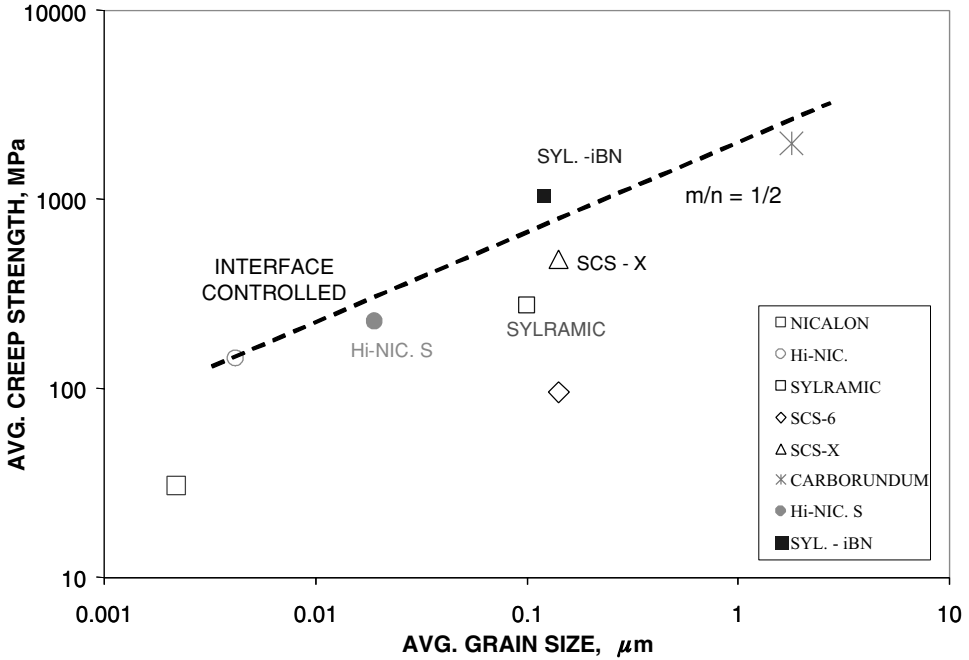


FIGURE 2. Creep strength of SiC fibers for strain limit of 0.4% at 1400°C for 10 hrs in air: open points = as-produced condition; closed points = after second phase removal.

of tests: stress rupture (constant stress and constant temperature), slow warm-up (constant stress, constant rate of temperature change), and fast-fracture (constant temperature and constant rate of stress change). It was found that by use simple thermal-activation theory, the rupture results of the three tests for each fiber type could be combined into a single LM master curve or q -map which describes the applied stress at rupture (fiber rupture strength) versus the time-temperature dependent parameter q given by

$$q \equiv Q_r/2.3R = T(\log t_r + 22). \quad (3)$$

Here Q_r is the effective stress-dependent activation energy for fiber rupture; T (kelvin) is the absolute temperature for the rupture test; and t_r (hours) is the fiber rupture time. Complete q -maps covering a wide range of temperatures and stresses are shown in Fig. 4a for two types of oxide fibers: Nextel 610 and Nextel 720, and for three types of SiC fibers: Hi-Nicalon, Sylramic, Sylramic-iBN. Here the curves represent best-fit averages of the fiber rupture times as measured for a ~ 25 mm gauge length.

The rupture results of Fig. 3a have many important basic and practical implications. First, on the basic level, all curves display approximately the same shape with increasing q ; that is, an initial section with a small negative slope (Region I), and a remaining section with a much larger negative slope (Region II). This behavior is typical of the rupture of monolithic ceramics, where as-produced flaws grow slowly in size (slow crack growth) in Region I; whereas in Region II, creep mechanisms aid in the more rapid growth of the same flaws or in the nucleation and growth of new micro-cracks and cavities. On the practical side,

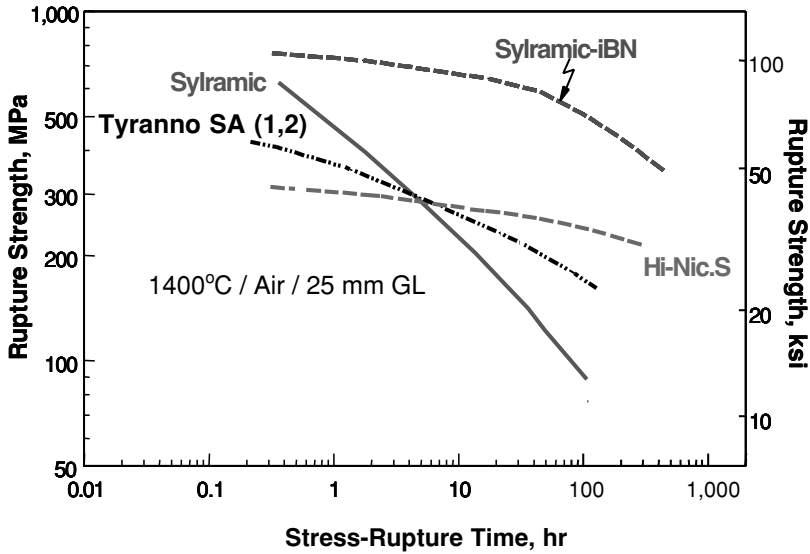


FIGURE 3. Best-fit rupture strength versus time curves for high-temperature SiC fibers tested at 1400°C in air under stress-rupture conditions at 25-mm gauge length.

the Fig. 3a curves indicate that fiber strength values throughout Region I depend directly on the fiber's as-fabricated strength at room temperature ($q \approx 7000$). That is, the entire Region I section moves up in strength when as-produced flaws are reduced in size or frequency. Alternatively, the section would move up or down if the test gauge length was smaller or greater, respectively, than the ~ 25 mm length used to generate the curves. In addition, Fig. 3a clearly indicates the greater thermostructural capability of the SiC fibers over the oxide-based fibers both in Regions I and II. The Region I advantage is related to the higher fracture toughness of SiC; while the Region II advantage is primarily due to slower diffusion processes in the SiC-based fibers. Finally, the Fig. 3 curves allow prediction of fiber rupture behavior if any four of the following five application variables are known: stress, stress rate, temperature, temperature rate, and time [16].

Besides single fibers, Larson-Miller master curves have also been generated for single multi-fiber tows of various ceramic fiber types [17]. Some of these are shown in Fig. 4b where again the environment is air and the gauge length is ~ 25 mm. Because tow strengths are typically controlled by the weakest fibers in the tow bundle, the tow LM curves are lower than the single fiber LM curves in Region I. However, in Region II the tows are generally stronger. The source of this strength reversal in Region II currently remains unknown.

One drawback of the LM approach for single fibers is that, as the rupture curves in Region II become steeper, the q -maps or LM curves begin to lose sensitivity in predicting fiber rupture strength at high temperatures. As discussed elsewhere [16], this is a consequence of fiber rupture being controlled by creep-induced flaws so that effective rupture energy Q_r is now controlled by the stress-independent fiber creep energy Q_c . Also the LM

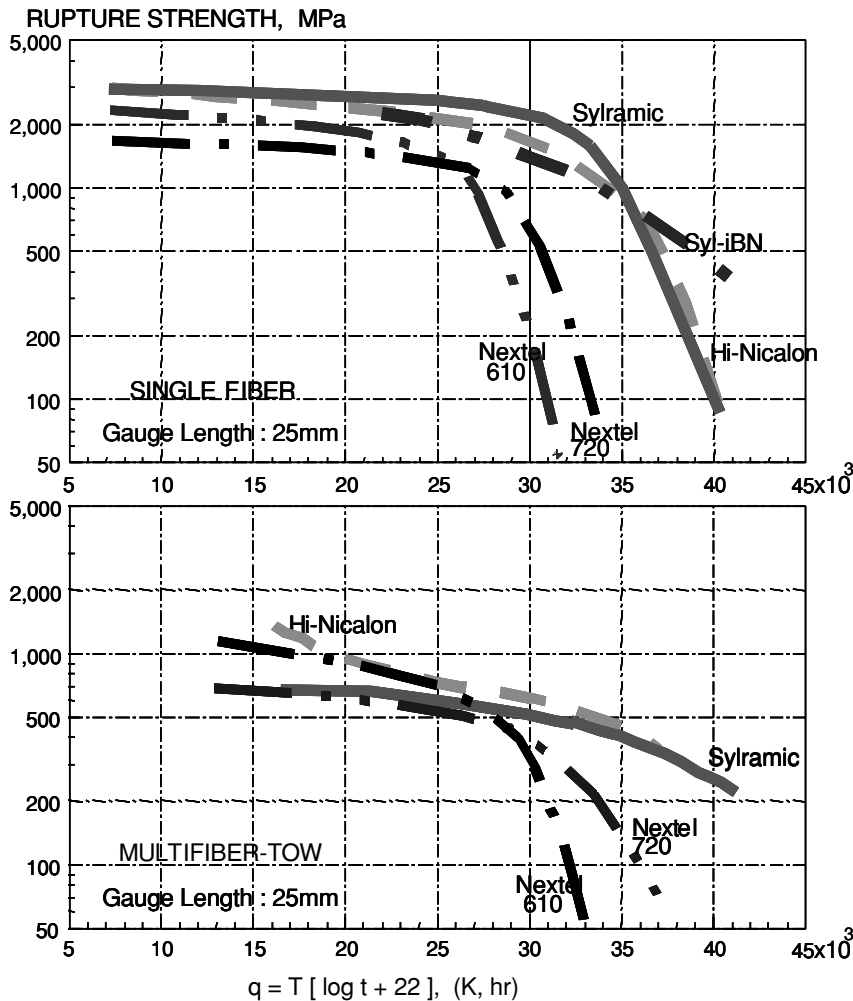


FIGURE 4. Best-fit Larson Miller or q -plot master curves measured in air for SiC and oxide fibers as (a) single fibers and (b) multi-fiber tows (T = kelvin, t = hours).

curves do not allow a direct quantitative assessment of fiber creep resistance. For example, the Hi-Nicalon and Sylramic fibers behave similarly in rupture at the high q values, but the Sylramic fiber creeps much less. To address these limitations, another convenient approach has been developed for describing SiC fiber rupture in the creep regime. This approach uses Monkman-Grant (MG) diagrams that plot at a given temperature the log of material rupture time versus the log of material creep rate at rupture [18]. For ceramic materials, the log-log results typically fall on one straight-line master curve. At higher temperatures, the MG lines usually retain the same slope, but rupture times increase with temperature for a given creep rate. Although SiC fibers appear to rupture in the primary creep stage (see

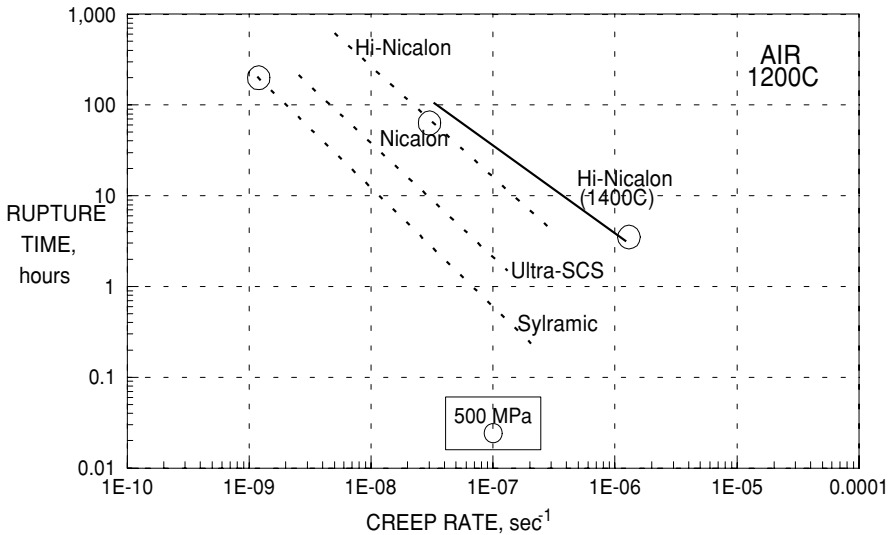


FIGURE 5. Best-fit Monkman-Grant lines measured in air for SiC single fibers at 1200°C and the Hi-Nicalon fiber at 1400°C.

Fig. 1), fairly consistent MG lines can still be constructed for the fibers based on their minimum creep rate at rupture. For example, Fig. 5 shows best-fit MG lines for average rupture time versus minimum creep rate (or instantaneous rate at rupture) for four SiC fibers at 1200°C in air [19]. Also included are the MG results for the Hi-Nicalon fiber tested at 1400°C in air.

As indicated in Fig. 5, the slopes for the MG lines for the various SiC-based fibers are similar to each other; and as temperature increases, rupture times (and strains) at a given creep rate also increase. However, *at a given creep rate and temperature*, rupture time data for the different SiC fiber types do not fall on the same MG line as might be expected from their somewhat similar compositions. This effect may be due to the anelastic component contributing to the measured creep rate, or to the observation that the smaller grained fibers, such as Hi-Nicalon, typically display larger rupture strains than the larger-grained fibers, such as Sylramic. On the practical side, this effect suggests that the rupture strains of the SiC fibers can possibly be improved by microstructural manipulation. Nevertheless, Fig. 5 shows that for a particular application temperature, one cannot select fiber rupture time independently of fiber creep rate. For example, up to 1200°C the only approach for obtaining a 1000-hour fiber lifetime is to assure that the application conditions do not create fiber creep rates more than $\sim 10^{-8} \text{ sec}^{-1}$ for the creep-prone fibers (Hi-Nicalon), or more than $\sim 10^{-9} \text{ sec}^{-1}$ for the more creep-resistant fibers (Sylramic).

In general, the maximum temperature/time/stress capability of the more creep-prone fibers is limited by the fiber tendency to display excessive creep strains (for example, $> 1\%$) before fracture. On the other hand, the temperature/time/stress capability of the more creep-resistant fibers is limited by fiber fracture at low creep strains ($< 1\%$), the values of which are often dependent on the environment. These limitations are illustrated in Table 3, which shows the approximate upper use-temperature for some SiC fibers, as determined from the

TABLE 3. 1000-hr upper use-temperatures for SiC ceramic fibers as estimated from single fiber creep-rupture results in air (and argon)

Fiber Stress 1000-Hr Limit Condition	100 MPa		500 MPa	
	1% Creep	Fiber Fracture*	1% Creep	Fiber Fracture*
Non-Stoichiometric Types				
Tyranno Lox M	1100°C	1250°C	<1000°C	1100°C
Tyranno ZMI, Nicalon	1150°C (1150°C)	1300°C (1250°C)	1000°C (1000°C)	1100°C (1100°C)
Hi-Nicalon	1300°C (1300°C)	1350°C (1300°C)	1150°C (1150°C)	1200°C (1150°C)
Near-Stoichiometric Types				
Tyranno SA	1350°C (1300°C)	> 1400°C (1400°C)	1150°C (NA)	1150°C (1150°C)
Hi-Nicalon	(NA)	> 1400°C	NA	1150°C
Type S		(1400°C)	(NA)	(1150°C)
Sylramic	(NA)	1350°C	(NA)	1150°C
	(NA)	(1250°C)	(NA)	(1150°C)
Sylramic-iBN	(NA)	> 1400°C (1300°C)	NA (NA)	1300°C (1150°C)
Ultra SCS			1350°C	>1400°C

* For ~25 mm gauge length.

single-fiber creep and rupture data discussed above. These upper use-temperatures were determined based on the assumption that the maximum temperature limiting condition occurred either when the fiber creep strain exceeded 1% in 1000 hours or when the fiber fractured in 1000 hours. Fiber stresses of 100 and 500 MPa were assumed, which are typical of the range of stresses experienced by fibers within structural CMC. A “not applicable” (NA) notation in the table indicates that the more creep-resistant fibers fractured before reaching a creep strain of 1%.

To put the rupture behavior of SiC fibers in further perspective, Fig. 6 compares the estimated 1000-hr upper use-temperatures for both commercially available oxide and SiC ceramic fibers based on single fiber rupture data at 500 MPa in air. These upper use-temperatures clearly indicate the greater thermostructural capability of the SiC fibers over the oxide fibers. Another important observation is that the fracture-limited upper use-temperatures of the more creep-resistant fibers are not measurably better than those of their more creep-prone counter-part fibers; e.g., compare Hi-Nicalon Type S versus Hi-Nicalon, and Tyranno SA versus Tyranno Lox M. Also as expected, the stoichiometric and purer SiC fiber types display the best temperature capability, with the Sylramic-iBN type currently the best polymer-derived fiber type in this regard. However, some of the more creep-resistant fiber types display better behavior in air than argon, with the Sylramic fiber types showing the largest difference [20]. This environmental effect can be attributed in part to a measurable reduction in intrinsic creep rate for some fiber types in air [20], and in part to reaction with oxygen to form a thin silica layer on the fiber surface. This layer minimizes vaporization of thermally unstable phases and also is capable of by blunting surface flaws,

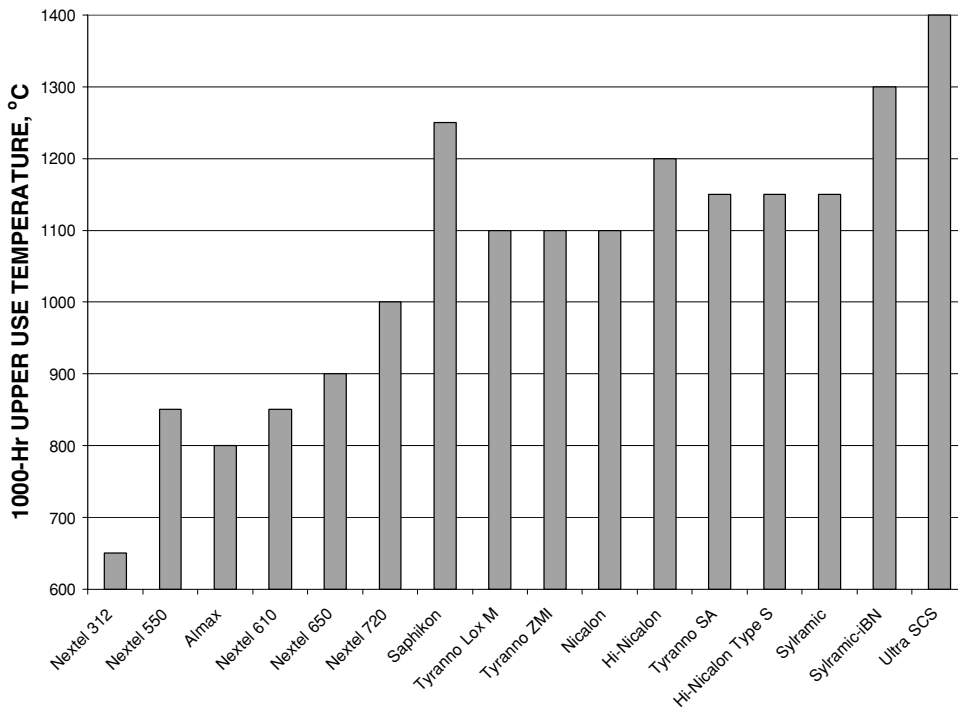


FIGURE 6. Estimated 1000-hour upper use-temperatures for rupture of small and large-diameter single ceramic fibers at 500 MPa in air at 25-mm gauge length.

thereby increasing the creep-rupture strain of all fiber types by as much as 100%. For CMC service under oxidizing conditions, this environmental effect can be important, since air may be the effective fiber environment if the CMC matrix is cracked and inert gas the effective environment if the matrix is uncracked.

Besides potential environmental effects on SiC fiber creep and rupture, one should also realize that the fiber conditions within a CMC during high-temperature application could be considerably different than those employed during simple stress rupture testing. For example, the condition of tensile stress being held constant both in time and along the fiber length will probably never exist during CMC application due to fiber curvature induced by the fiber architecture and to the typical occurrence of CMC matrix cracking, where fiber stresses are highest within the matrix cracks and then drop off within the intact segments of the matrix. It should also be clear that under these CMC conditions, fiber gauge length is considerably smaller than the 25 mm length typically used for the stress rupture testing. Thus, using the data presented here to model SiC fiber high-temperature mechanical behavior in an accurate quantitative manner is probably not warranted at the present time. Nevertheless, as shown by available SiC fiber-reinforced CMC data discussed in other chapters of this book [21, 22], the *relative differences* between various ceramic fiber types as described in this section are generally observed in the high-temperature fiber-controlled properties of the CMC.

4.3. *Properties needed for CMC Applications*

Composite applications for SiC fibers typically center on CMC for high-temperature structural applications ($>1100^{\circ}\text{C}$), where lower creep and grain-growth rates in comparison to metallic alloys and oxide fiber composites allow better dimensional stability and strength retention under the combined conditions of temperature and stress. The SiC fibers can also provide CMC with greater thermal and electrical conductivity, higher as-produced strength, and lower density. However, under oxygen and moisture-containing environmental conditions, the exposed surfaces of Si-based fibers will degrade slowly due to silica growth and surface recession. Nevertheless, silica is among the most protective of scales, so that in a general sense, SiC fibers display good oxidation resistance in the short term. It follows then that SiC-based fibers are generally preferred for CMC applications that require (1) structural service under environmental conditions that minimally expose the fibers to oxygen and (2) upper use temperatures higher than possible with oxide/oxide CMC or state-of-the-art metallic alloys. Minimal oxygen exposure is typically achieved by incorporating the fibers in dense protective matrices of similar composition and thermal expansion that can remain un-cracked after CMC fabrication, such as in SiC/SiC composites.

Today extensive developmental efforts are underway to utilize SiC/SiC CMC in land- and aero-based gas turbine engines for hot-section components that require service for many hundreds of hours under combustion gas environments [21, 22]. For the purpose of achieving high performance high-temperature SiC/SiC components, CMC experience has shown that a variety of issues exist which relate to retaining the as-produced properties of the reinforcing SiC fibers during component fabrication and service. Many of these issues arise in the fabrication stage during the various steps of (1) shaping the continuous length fibers into architectural arrays or preforms that yield near net-shape component structures, (2) coating the fibers within the architectural preforms with thin fiber coatings or interphase materials that are required for matrix crack deflection, and (3) infiltrating the coated-fiber architectural preforms with SiC-based matrix material, which is often performed at temperatures of 1400°C and above. Issues also arise during CMC service when the SiC matrix may crack due to unforeseen stresses. Since these issues dictate additional second-level property requirements for the SiC fibers, the remainder of this section discusses these property needs in more detail and the ability of current SiC fibers to achieve them.

For the CMC architecture formation step, some issues that can arise during fiber shaping include fiber-fiber abrasion within the multi-fiber tows and excess fiber bending stresses, which may even cause fiber fracture during this step or provide new fiber surface flaws and residual bending stresses in the architecture that eventually cause premature fiber fracture during component structural service. Fiber-fiber abrasion can be minimized by fiber types with surface layers that are smooth and have abrasion resistant compositions such as carbon or boron nitride. Sizing can also be helpful in this regard, but since the sizing typically covers the outer fibers of the tow, it is probably not as effective as abrasion-resistant coating layers on each fiber surface. Likewise, fiber bending stresses can be minimized by fiber types that have small diameters and low elastic moduli. Thus for architecture formation, as well as for low acquisition cost, the first-generation polymer-derived fibers such as Nicalon and Tyranno Lox M are generally the first choice for component fabrication due to their carbon-rich surfaces, small grain size or surface roughness, and lower elastic moduli. But as described above, these fiber types are not desirable for the higher temperature components.

Since achieving these components necessitates use of high-performance SiC fibers with their concomitant high modulus and large surface roughness, current approaches for high-performance SiC/SiC component are focusing on (1) near-stoichiometric SiC fiber types with either carbon-rich surfaces (Hi-Nicalon Type S) or BN-rich surfaces (Sylramic-iBN), and (2) textile formation processes that provide abrasion-resisting liquids on the fiber surfaces during the architecture formation step.

During the CMC fabrication step in which chemical vapor infiltration (CVI) is typically used to deposit thin BN or carbon-containing crack-deflecting interfacial coatings on the fiber surfaces, potential fiber strength-degrading issues include the risk that chemically aggressive gases such as halogens, hydrogen, or oxygen may reach the SiC fiber surface before the protective BN and carbon interfacial materials are formed. The halogens and hydrogen have been demonstrated to cause fiber weakening by surface flaw etching [23]; whereas oxygen allows the growth of silica on the fiber surfaces, which in turn causes strong mechanical bonds to be formed between contacting fibers in the fiber architectures [24]. The detrimental consequence of fiber-fiber bonding is that if one fiber should fracture prematurely, all others to which it is bonded will prematurely fracture, causing composite fracture or rupture at stresses much lower than those that would be needed if the fibers were able to act independently. This oxidation issue is also serious during SiC/SiC service where the possibility exists that cracks may form in the SiC matrix, thereby allowing oxygen from the service environment to reach the reinforcing fibers. Because of the high reactivity of carbon with oxygen above $\sim 500^{\circ}\text{C}$ and subsequent volatility of the bi-products, cracking of the matrix can be especially serious for those SiC fiber types with carbon-rich surfaces or for fibers and interphase materials based on carbon. For this reason, many SiC/SiC component development programs in the U.S. are utilizing BN-based interfacial coatings, as well as the Sylramic-iBN SiC fiber type with its in-situ grown BN surface layer [22].

Finally, during the CMC matrix formation step, current SiC/SiC fabrication trends are progressing toward SiC-based matrices that are formed at 1400°C and above in order to improve matrix and composite creep-rupture resistance and thermal conductivity [22]. In these cases, the matrix formation times and temperatures are high enough to cause microstructural changes and strength degradation in the non-stoichiometric SiC fibers that are produced at temperatures below 1400°C . These effects can also occur in a near-stoichiometric type if its maximum production temperature is below that for matrix processing. Thus the high performance SiC fibers with the highest production temperatures (see Table 1) are generally preferred for these new matrix formation approaches at higher temperatures.

5. SUMMARY AND CONCLUSIONS

This paper has examined the current state of experimental and mechanistic knowledge concerning the production methods, microstructures, physical properties, and mechanical properties at room and high temperature for a variety of fine-grained SiC-based ceramic fibers of current interest for CMC reinforcement. It has been shown (1) that good correlations exist between the fiber production methods, microstructures, and properties, and (2) that fiber production methods over recent years have significantly improved the key fiber properties needed for implementing SiC fibers in advanced high-temperature CMC components. In particular, these methods have eliminated such performance degrading impurities as excess

oxy-carbides, carbon, boron, and silicon to yield dense, high purity, near-stoichiometric SiC fibers with grain sizes optimized for fiber tensile strength, creep-rupture resistance, thermal conductivity, and intrinsic temperature capability. However, along with these advances, fiber acquisition costs have risen to the point that SiC fiber use in the near term may be limited only to those applications where their usage is enabling, rather than enhancing.

Because of their lower atomic diffusion, higher fracture toughness, lower density, and higher thermal conductivity in comparison to oxide fibers, pure near-stoichiometric SiC fibers are currently the preferred reinforcement for CMC products that are required to operate for long times at temperatures greater than state-of-the-art metal alloys ($>1100^{\circ}\text{C}$). While reduction in production costs and further improvement in high-temperature creep-rupture resistance are on-going developmental issues for future SiC-based fibers, another important issue is improvement of the fiber surfaces against environmental attack. In this area, possibilities exist for the development of oxidation-resistant fiber coatings that are deposited on tows after fiber processing, or better yet in terms of cost reduction, are formed in-situ during fiber production. These new coating approaches should also be beneficial for reducing fiber abrasion and strength degradation during the complex weaving and braiding processes typically needed for some CMC products. As described here, the new Sylramic-iBN fiber type with an in-situ grown BN layer goes a long way in this direction, as well as providing most of the other key properties needed for the fiber reinforcement of high-temperature SiC/SiC composites.

6. REFERENCES

1. J.A. DiCarlo and S. Dutta, Continuous Ceramic Fibers for Ceramic Composites, *Handbook On Continuous Fiber Reinforced Ceramic Matrix Composites*, Eds R. Lehman, S. El-Rahaiby, and J. Wachtman, Jr., CIAC, Purdue University, West Lafayette, Indiana, 1995, p. 137–183.
2. *Ceramic Fibers and Coatings*, National Materials Advisory Board, Publication NMAB-494, National Academy Press, Washington, D.C., 1998.
3. A.R. Bunsell and M-H. Berger, *Fine Ceramic Fibers*, Marcel Dekker, New York, 1999.
4. H. Ichikawa and T. Ishikawa, Silicon Carbide Fibers (Organometallic Pyrolysis), *Comprehensive Composite Materials*, Vol. 1, Eds. A. Kelly, C. Zweben, and T. Chou, Elsevier Science Ltd., Oxford, England, 2000, p. 107–145.
5. D.M. Wilson, J.A. DiCarlo, and H-M. Yun, Ceramic Fibers, *ASM Handbook, Volume 21 Composites*, ASM International, Materials Park, Ohio, 2001, pp. 46–50.
6. J.A. DiCarlo and H-M. Yun, Microstructural Factors Affecting Creep-Rupture Failure of Ceramic Fibers and Composites, *Ceramic Transaction*, **99**, 1998, p. 119–134.
7. H-M. Yun and J.A. DiCarlo, Comparison of the Tensile, Creep, and Rupture Strength Properties of Stoichiometric SiC Fibers, *Cer. Eng. Sci. Proc.*, **20** [3], 1999, p. 259–272.
8. J.A. DiCarlo, Property Goals and Test Methods for High Temperature Ceramic Fibre Reinforcement, *Ceramics International* **23** (1997) 283.
9. R. Bodet, X. Bourant, J. Lamon, and R. Naslain, Tensile Creep Behavior of A Silicon-Carbide-Based Fibre with Low Oxygen Content, *J. Mater. Sci.*, **30** (1995), 661–677.
10. H-M. Yun, J.C. Goldsby, and J.A. DiCarlo, Effects of Thermal Treatment on Tensile Creep-Rupture Behavior of Hi-Nicalon SiC Fibers, *Cer. Eng. Sci. Proc.*, **16** [5] (1995), 987–996.
11. J.A. DiCarlo, Creep of Chemically Vapour Deposited SiC Fibers, *J. Mater. Sci.*, **21** (1986), 217–224.
12. G.N. Morscher, H-M. Yun, and J.C. Goldsby, Bend Stress relaxation and Tensile Primary Creep of a Polycrystalline α -SiC Fiber, *Plastic Deformation of Ceramics*, eds. R. Bradt, C. Brooks, and J. Routbort (New York: Plenum Publishing, 1995), pp. 467–478.
13. A.S. Nowick and B.S. Berry, *Anelastic Relaxation in Crystalline Solids* (New York: Academic Press, 1972).

14. J.A. DiCarlo and H-M. Yun, Creep of Ceramic Fibers: Mechanisms, Models, and Composite Implications, *Creep Deformation: Fundamentals and Applications*, eds. R.S. Mishra, J.C. Earthman, and S.V. Raj, The Minerals, Metals, and Materials Society, Warrendale, PA, 2002, pp. 195–208.
15. H-M. Yun, J.C. Goldsby, and J.A. DiCarlo, Tensile creep and Stress-Rupture Behavior of Polymer Derived SiC Fibers”, *Ceramic Transactions*, **46** (1994), 17–28.
16. H-M. Yun and J.A. DiCarlo, Time/Temperature Dependent Tensile Strength of SiC and Al₂O₃-Based Fibers”, *Ceramic Transactions*, **74**, 1996, p. 17–26.
17. H-M. Yun and J.A. DiCarlo, Thermo-mechanical Properties of Ceramic Fibers for Structural Ceramic Matrix Composites, *Proceedings of CIMTEC '02*, Florence, Italy, 2002.
18. F.C. Monkman, and N.J. Grant, An Empirical Relationship between Rupture Life and Minimum Creep Rate”, *Proc. ASTM*, **56** (1956), 593–620.
19. J.A. DiCarlo and H-M. Yun, “Creep and Stress Rupture Behavior of Advanced SiC Fibers,” *Proceedings of ICCM-10, vol. VI* (Cambridge, England: Woodhead Publishing Limited, 1995), 315–322.
20. H-M. Yun, J.C. Goldsby, and J.A. DiCarlo, Environmental Effects on Tensile Creep and Rupture Behavior of Advanced SiC Fibers, *Ceramic Transactions*, **57** (1995), 331–336.
21. G.S. Corman and K.L. Luthra, Silicon Melt Infiltrated Ceramic Composites (HiPerCompTM), in *Handbook of Ceramic Composites*, N.P. Bansal, Ed., Kluwer Academic Publishers, Boston, MA, 2004, pp. 99–115.
22. J.A. DiCarlo, H.M. Yun, G.N. Morscher, and R.T. Bhatt, SiC Fiber-Reinforced SiC Matrix Composites for Thermostructural Applications to 1200°C and Above, in *Handbook of Ceramic Composites*, N.P. Bansal, Ed., Kluwer Academic Publishers, Boston, MA, 2004, pp. 77–98.
23. F. Rebillat, A. Guette, L. Espitalier, and R. Naslain, Chemical and Mechanical Degradation of Hi-Nicalon and Hi-Nicalon S Fibers under CVD/CVI BN Processing Conditions, *High Temperature Ceramic Matrix Composites III*, The Ceramic Society of Japan, 1998, pp. 31–34.
24. Morscher, G.N., Tensile Stress Rupture of SiC/SiC Minicomposites with Carbon and Boron Nitride Interphases at Elevated Temperatures in Air, *J. Am. Ceram. Soc.* **80** [8], 1997, pp. 2029–2042.



<http://www.springer.com/978-1-4020-8133-0>

Handbook of Ceramic Composites

Bansal, N.P. (Ed.)

2005, X, 554 p., Hardcover

ISBN: 978-1-4020-8133-0